TISSUE ENGINEERING
Volume 12, Number 10, 2006

Mesenchymal Stem Cells Enhance Angiogenesis in Mechanically Viable Prevascularized Tissues via Early Matrix Metalloproteinase Upregulation

CYRUS M. GHAJAR, M.S.,[1] KATHERINE S. BLEVINS, B.S.,[1] CHRISTOPHER C.W. HUGHES, Ph.D.,[1,2] STEVEN C. GEORGE, M.D., Ph.D.,[1,3] and ANDREW J. PUTNAM, Ph.D.[1,3]

ABSTRACT

Angiogenesis, the sprouting of new blood vessels from existing vasculature, is a complex biological process of interest to both the treatment of numerous pathologies and the creation of thick engineered tissues. In the context of tissue engineering, one potential solution to the diffusion limitation is to create a vascular network *in vitro* that can subsequently anastomose with the host after implantation, allowing the implantation of thicker, more complex tissues. In this study, the ability of endothelial cells to sprout and form stable vascular networks in 3-dimensional (3D) fibrin matrices was investigated as a function of matrix density in a prevascularized tissue model. The results demonstrate that while increasing matrix density leads to a nearly 7-fold increase in compressive stiffness, vascular sprouting is virtually eliminated in the most dense matrix condition. However, the addition of human mesenchymal stem cells (HMSCs) to the denser matrices reverses this effect, resulting in an up to a 7-fold increase in network formation. Although the matrix metalloproteinases (MMPs) MMP-2, MMP-9, and MT1-MMP are all upregulated early on with the addition of HMSCs, MT1-MMP appears to play a particularly important role in the observed angiogenic response among these proteases. This study provides a means to design stiffer prevascularized tissues utilizing naturally derived substrates, and its results may yield new mechanistic insights into stem cell–based angiogenic therapies.

INTRODUCTION

ANGIOGENESIS, the sprouting and growth of a branching capillary network into a previously avascular tissue, is a complex and dynamic process that depends on the interplay of soluble factors and insoluble cues from the extracellular matrix (ECM).[1] This multistep process involves degradation of the basement membrane and subjacent matrix around a preexisting vessel, endothelial cell migration and proliferation, and differentiation into functional tubular networks, which requires stabilization by neighboring pericytes and the reformation of basement membrane.[2] Matrix metalloproteinases (MMPs), a family of Zn^{2+}-binding and Ca^{2+}-dependent endopeptidases,[3] play a critical role by degrading the ECM to facilitate the initial steps of angiogenesis.

The role of the ECM in angiogenesis is of particular interest to 2 emerging fields of research: therapeutic angiogenesis and tissue engineering. A number of pathologies are characterized by poor blood vessel growth and, as a result, inadequate nutrient delivery.[4,5] The focus of angiogenic therapies is to enhance vessel growth into these tissues to prevent progression of the pathology. Tissue engineering was developed, in part, to generate new tissue

[1]Department of Biomedical Engineering, University of California-Irvine, Irvine, California.
[2]Department of Molecular Biology and Biochemistry, University of California-Irvine, Irvine, California.
[3]Department of Chemical Engineering and Materials Science, University of California-Irvine, Irvine, California.

when these therapies fail. However, the field has seen limited success owing to an inability to construct tissues greater than 200 μm in thickness.[6] A potential solution to overcome this limitation is to construct a prevascularized tissue *in vitro* which then anastomoses with the host vasculature upon implantation. This approach has been attempted with varying success,[7–10] and systems employing naturally derived ECM proteins (e.g., fibrin or collagen) may lack the mechanical integrity necessary to withstand local forces present at the implant site. The simplest method of enhancing the mechanical properties of these matrices is to increase the concentration of matrix protein; however, doing so increases the density of the tissue, mimicking fibrosis, and adversely affects angiogenesis.

While the effect of ECM density[11] and mechanical properties[12] on angiogenesis is well documented in 2-dimensional systems, those systems do not necessarily recapitulate the 3-dimensional (3D) *in vivo* environment. Moreover, the majority of 3D studies conducted *in vitro* lack a robust system capable of sustaining capillary-like structures long term.[13,14] Thus, we have adapted a system for this study that utilizes human umbilical vein endothelial cells (HUVECs) coated on microcarrier beads embedded within a fibrin matrix that form stable capillary-like structures when cultured in the presence of fibroblasts.[15,16]

We employed this system to characterize how increasing fibrinogen concentration affects the physicochemical properties of the fibrin matrix, and demonstrate that increasing matrix density severely diminishes capillary formation and growth both short and long term. Adding human mesenchymal stem cells (HMSCs) throughout the culture was found to upregulate MMP-2, MMP-9, and membrane type-1 (MT1)-MMP early on (within 3 days), leading to significantly increased network formation. Our data support the growing body of work implicating the importance of both soluble (e.g., MMP-2) and membrane-type MMP expression to angiogenesis.[3,13,17–19] The results of this study suggest strategies to create prevascularized tissues within mechanically viable matrices and perhaps provide evidence for the use of HMSCs as a therapeutic approach to stimulate angiogenesis.

EXPERIMENTAL PROTOCOL

Characterization of fibrin gel properties

The static mechanical properties of the fibrin gels were assessed via unconfined compressive tests. Fibrin gels were fabricated by dissolving the appropriate amount of fibrinogen (Sigma-Aldrich, St. Louis, MO) in endothelial growth media (EGM-2; Clonetics, East Rutherford, NJ) to reach the desired concentration. One milliliter of this solution was then mixed with 20 μL of thrombin (50 U/mL, Sigma) and pipetted on top of a steel disk sitting flush on the bottom of a custom Teflon mold. After the sample was left at room temperature for 5 min, it was allowed to polymerize at 37°C for another 25 min before testing in order to mimic polymerization conditions when constructing fibrin tissues. At this juncture, the sample was removed by carefully cutting around the border of the well with a spatula and utilizing the steel disk beneath the sample to remove the gel from the well intact (necessary for the 2.5 mg/mL gels, and followed for the other samples to maintain uniformity). Sample diameter and thickness were immediately measured using a digital caliper. The sample was then placed at the center of the testing stage on a MTS Synergie 100 (MTS Systems, Eden Prairie, MN) with a 10 N load cell, and the test platen was carefully lowered until it just touched the top of the hydrogel. The TestWorks 4 software package was used to conduct the unconfined compressive test at a uniform deformation rate of 1 mm/min and a data acquisition rate of 10 Hz. Compressive modulus was extracted from the data by taking the slope of the initial linear region of the stress–strain curve.[20]

To visualize the network architecture of fibrin gels as concentration was varied, Oregon Green 488-conjugated fibrinogen (Molecular Probes, Eugene, OR) was mixed at a 1:1000 ratio with unlabeled fibrinogen of equal density as previously described.[21] The gel was polymerized and allowed to equilibrate overnight at 37°C in phosphate-buffered saline (PBS) before imaging. Images were captured using a Zeiss LSM 510 Meta confocal microscope (Carl Zeiss, Germany). Five such images were chosen at random per condition and analyzed with Adobe Photoshop by thresholding the intensity of the green channel to obtain the percentage of black pixels for each image. These values were averaged and used to generate a plot for porosity.

Cell culture

Normal human lung fibroblasts (NHLFs, ATCC, Manassas, VA) were cultured in Media 199 (Invitrogen Corporation, Carlsbad, CA) with 10% fetal bovine serum (FBS). Media were changed every 2 days and cells were harvested with trypsin–EDTA (Invitrogen). HMSCs (Cambrex, East Rutherford, NJ) were cultured in Dulbecco's modified Eagle medium (DMEM) (Invitrogen) supplemented with 10% FBS and 1% penicillin-streptomycin. HUVECs were isolated from freshly harvested umbilical cords. Collagenase type 1A (Sigma) digestion was performed at 37°C for 10 min to release endothelial cells from the vessel walls. After the umbilical vein was rinsed with Hank's balanced salt solution (Clonetics), the wash was collected and centrifuged. The remaining pellet was resuspended in EGM-2 without vascular endothelial growth factor (VEGF). All cells were plated in collagen-treated culture flasks. NHLFs and MSCs were used prior to passage 10, while HUVECs were used at passage 3.

Vascularized tissue assembly

Fibrin tissues were assembled as previously described.[7] Cytodex microcarrier beads (Sigma) were sterilized and

prepared for seeding by washing repeatedly with EGM-2 without VEGF. Ten thousand such beads (diameter ≈ 150 μm) were combined in 5 mL of EGM-2 (no VEGF) with 4×10^6 HUVECs and agitated periodically over 4 h in an inverted T-25 culture flask. After 4 h, 5 mL of fresh medium was added to the cell–bead mixture. The total volume was then transferred to a fresh T-25 and incubated in standard cell culture position.

The next day, a fibrinogen solution of the desired concentration (2.5 mg/mL, 5 mg/mL, or 10 mg/mL, based on desired experimental conditions) was prepared and sterile filtered. Five hundred microliters of this solution (with or without 5×10^4 HMSCs, depending on the experimental conditions) was mixed with approximately 100 HUVEC-coated beads and combined with 10 μL of thrombin (50 U/mL) in a single well of a 24-well plate to make one tissue. This process was repeated until the desired amount of tissues was generated. At this point, the tissues were left undisturbed for 5 min to allow the beads to settle at the bottom of the well before incubating for 25 min at 37°C and 5% CO_2 to encourage gelation. NHLFs were then plated (25K/well) on top of the fibrin gel.

Tissues were cultured in fully supplemented EGM-2. Medium was changed every 2 days. For the studies involving GM6001 (Calbiochem, San Diego, CA), a volume commensurate to the indicated molar concentration of the MMP inhibitor (diluted in dimethyl sulfoxide) was added to the well after each media change. Vehicle control studies were performed (data not shown) to ensure that the maximum volume of diluting solution used had no effect, adverse or otherwise, on vascular sprouting.

Images and quantification of total network length

Tissues were imaged at three time points post-assembly (days 7, 14, and 21) via brightfield phase-contrast microscopy (Nikon TE300 microscope; Nikon, Melville, NY) using Metamorph software (Universal Imaging/Molecular Devices Corporation, Union City, CA). At least 5 beads per condition were randomly imaged at low power (4×). Beads were eliminated from consideration if vessels sprouting from the bead were not greater in length than the radius of the given bead (to discount those beads that were insufficiently coated by HUVECs) or if the vessels anastomosed with those of a neighboring bead (since this would complicate quantification of network length). The resulting images were then saved as high-resolution files (*.tif).

The subsequent images for each condition and time point (160 total) were then randomized. Vessel segments for each bead were traced, quantified, and totaled using image processing software (Scion Image; Scion Corporation, Frederick, MD) to generate values for total network length. These values were measured directly from the high-resolution images by 2 different research personnel ''blinded'' to the experimental conditions. This resulted in 2 total network length values for each quantified bead, which were then averaged. Five such values were then averaged per condition and used to generate the data presented in the graphs for Figs. 3–6.

Gelatin zymography

Gelatin zymography was performed as previously described[13] at 4 separate time points per condition: days 3, 7, 14, and 21. For each condition, 2 fibrin tissues, each containing approximately 100 HUVEC-coated beads, were digested and pooled together. Fibrin tissues were digested in the following manner: after aspirating EGM-2, 100 μL of ice-cold Garner buffer (50 mM Tris, pH 7.5; 150 mM NaCl; 1 mM phenylmethylsulfonyl fluoride; 1% Triton X-100) was added to the well. The contents of the well were then removed and placed within a 5-mL centrifuge tube. Two cycles of 15-s sonication (10 W) followed by 30 s of vortex-mixing were performed on each sample to liquefy the gel and lyse the cells within. Any remaining solids were removed by centrifugation at 14,000 rpm for 10 min and isolating the supernatant from the resulting pellet. Bicinchoninic acid assay (Pierce Biotechnology, Rockford, IL) was utilized to determine the protein concentration of the supernatant.

Novex zymogram gels (10% Tris-glycine gel with 0.1% gelatin) (Invitrogen) were loaded with equal protein amounts and separated under nonreducing conditions. The gels were then washed for 20 min in Tris-buffered saline (TBS) with 2.5% Triton X-100 and then incubated at 37 °C for 20 h in enzyme incubation buffer (25 mM Tris, pH 8; 2.5 mM $CaCl_2$; 0.02% NaN_3). After the wash and incubation were repeated, gels were stained with Coomassie brilliant blue for 1 h and destained twice for 15 min each in 10% acetic acid and 20% ethanol. MMP-2 and MMP-9 bands for each sample were identified by running a MMP-2 and MMP-9 standard (Chemicon, Temecula, CA) in a lane of each gel. Band intensities were obtained by imaging the gel using the Quantity One software package (Bio-Rad, Hercules, CA) and analyzing bands using image processing software (NIH Image; National Institutes of Health, Bethesda, MD). Resulting intensity values were normalized by the corresponding intensity of the 2.5 mg/mL sprouting condition for each gel. Normalized values for each condition were then averaged to allow for statistical comparisons.

Western blot analysis

Western blot analysis of the levels of the membrane associated MMP, MT1-MMP, was conducted on samples harvested (using the same techniques as those described earlier for gelatin zymography) on days 3, 7, 14, and 21. After briefly boiling, equal amounts of protein (40 μg) from tissue lysates were electrophoresed in a 10% Tris-glycine gel (Novex/Invitrogen) under reducing conditions. The proteins were then transferred to a poly(vinylidine fluoride) membrane and probed with a polyclonal anti-MT1-MMP

antibody (1:250) (Santa Cruz Biotechnologies, Santa Cruz, CA). After washing, the membrane was incubated with a horseradish peroxidase–conjugated secondary antibody (1:5000). Membranes were detected via an enhanced chemiluminescence detection system. Identity of MT1-MMP band was verified with MCF-7 lysate (Santa Cruz Biotechnologies), as suggested by the manufacturer. The resulting blots were scanned and imported into NIH Image (National Institutes of Health) in order to perform densitometry. Bands were processed as described previously for the zymograms.

Statistical analyses

Statistical analyses were performed using InStat 2.01. Data are reported as means ± standard deviations. All statistical comparisons were made by performing a one-way analysis of variance (ANOVA), followed by a Student–Newman–Keuls multiple comparisons test to judge significance between two data sets at a time. *P* values less than 0.05 are considered statistically significant.

RESULTS

HUVECs form extensive vascular networks by day 21 when cultured within fibrin gels in the presence of NHLFs

Previous studies have shown that HUVECs will sprout, proliferate, migrate, and form branching capillary networks in a fashion similar to capillaries *in vivo* when cultured in fibrin gels in the presence of fibroblasts.[16] Fibroblasts provide soluble signals to stabilize these structures,[16] resulting in an environment that facilitates the growth of vessels into vast, anastomosing networks beyond 3 weeks (Fig. 1A). The optimal concentration of fibrin for this assay, 2.5 mg/mL, is nearly that of the circulating concentration of fibrinogen in human blood.[22] Immunofluorescent staining of these cultures demonstrates that extensive cell migration from the microcarrier bead occurs after 7 days, resulting in multinucleated structures with contiguous actin cytoskeletons formed in the direction of vessel branching (Fig. 1B). Figure 1C further demonstrates that capillary sprouting in this system requires tunneling through the fibrin ECM, and serves as an impetus to explore how changing the properties of the matrix (green channel) affects this process. The notion that ECM degradation products are critical to angiogenesis[23] further implicates a role for MMPs.

Confocal analysis through multiple parallel focal planes of cultures stained for F-actin and vinculin (a protein that localizes at the site of focal adhesions, or contact sites between the cell and ECM) was used to visualize the tubular nature of structures. Figure 1D–F shows 3 planes of one such stack (*Z*-direction) at the base (Fig. 1D), middle (Fig. 1E), and apex (Fig. 1F) of a capillary. The presence of nuclei, F-actin, and vinculin is evident throughout the basal and apical sections of the capillary, while they are clearly present only along the border in the middle slice, demonstrating that HUVECs have differentiated into lumen-containing structures.

Increasing fibrinogen concentration results in enhanced compressive modulus and reduced network porosity

Because variations in fibrinogen concentration impact both the mechanical properties and the pore size of fibrin gels, it is essential to establish how these physical properties change as the fibrin matrix density is manipulated. Accordingly, unconfined compression tests (summarized in Fig. 2A) were conducted on gels with initial fibrinogen concentrations of 2.5, 5, and 10 mg/mL, resulting in mean (± SD) modulus values of 1.29 ± 0.33, 4.06 ± 0.40, and 8.99 ± 1.06 kPa, respectively. (These values are slightly below those reported for skeletal muscle tissue,[24] suggesting the physiological relevance of these fibrin matrices for soft tissues.) This range yielded matrices that were nearly 3 (5 mg/mL) and 7 (10 mg/mL) times stiffer than the baseline (2.5 mg/mL) condition.

Fluorescently labeled fibrinogen was used to visualize changes in network architecture that occurred with increasing fibrinogen concentration. High-power confocal images of each condition (Fig. 2B–D) demonstrate an inverse relationship between matrix density and porosity. By thresholding an image, a simple comparison of green to black pixels was possible, allowing the calculation of relative network porosity. These data (Fig. 2E) confirmed that increasing fibrinogen concentration results in a less porous matrix (26.46%, 20.32%, and 9.66% porosity for 2.5 mg/mL, 5 mg/mL, and 10 mg/mL gels, respectively).

Increasing matrix density restricts capillary sprouting through a mechanism that involves reduced early expression of MT1-MMP

To investigate the effects of matrix density on capillary sprouting, HUVEC-coated beads were cultured in 2.5, 5, and 10 mg/mL fibrin gels. The effect of increased matrix density was visible by week one (not shown), and was exaggerated by week three (Fig. 3A–C). Quantification of these networks (Fig. 3D) demonstrated a significant decrease in network length as fibrinogen concentration increased, culminating in a highly significant difference between all conditions by day 21 (mean network length for the 5 mg/mL condition was 38.7% of the baseline case, while the 10 mg/mL condition was only 2.7%).

To decipher a mechanism underlying this response, we investigated the activity of MMP-2 and MMP-9, secreted MMPs previously shown to be important for angiogenesis and fibrinolysis in alternate systems.[17,18] Activity of these MMPs was examined via gelatin zymography, a technique that allows

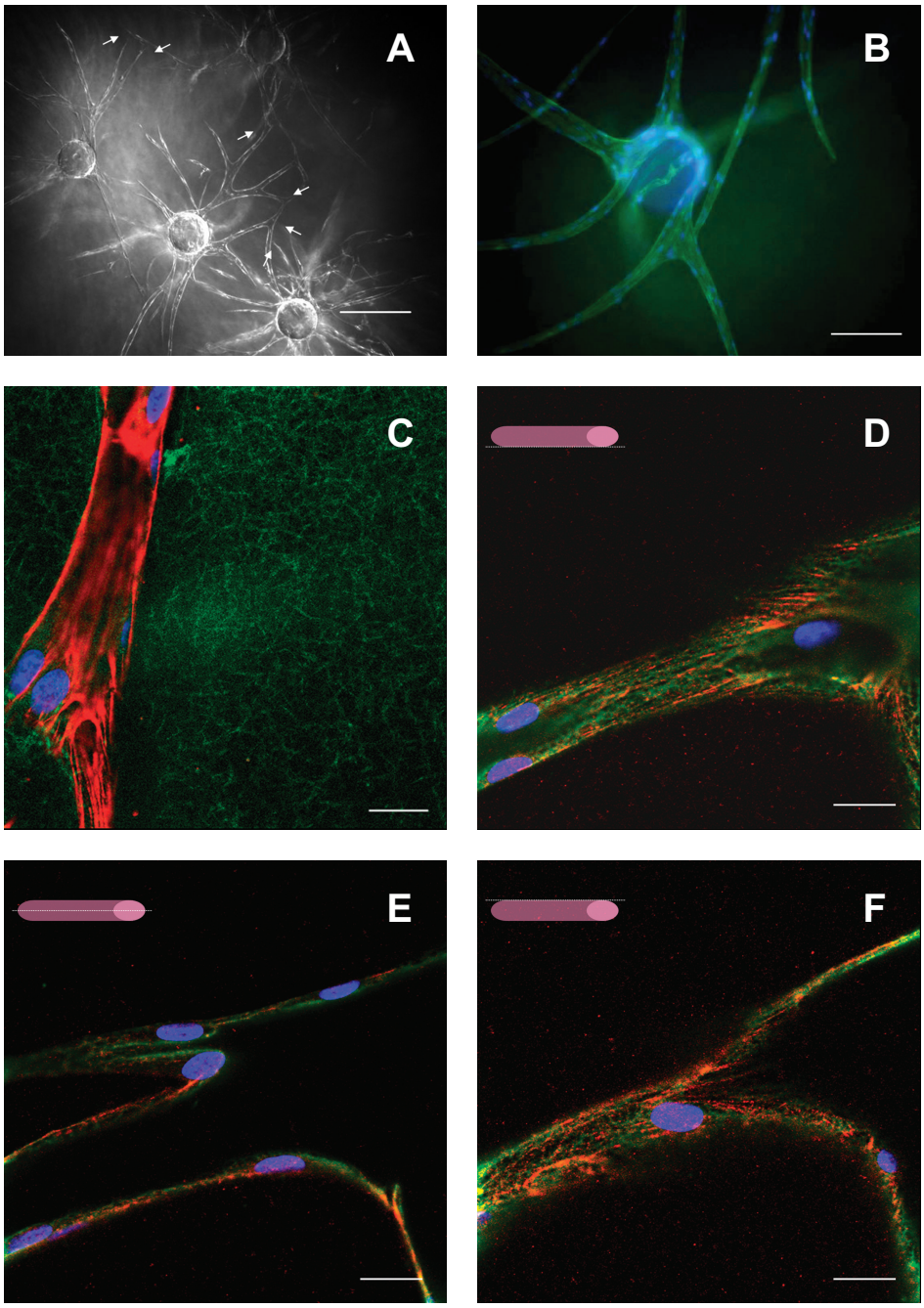

FIG. 1. HUVECs form capillary-like networks when cultured within fibrin gels. (**A**) Day 21 image of 2.5 mg/mL fibrin culture demonstrates formation of numerous anastomoses between neighboring beads (indicated with white arrows). Scale bar = 500 μm. (**B**) Fluorescent staining of day 7 2.5 mg/mL culture with Oregon Green 488–conjugated phalloidin and 4′,6-diaminidino-2-phenylindole (DAPI) were visualized via fluorescent microscopy. Scale bar = 200 μm. (**C**) High-magnification confocal image of day 7 culture. Tubular structures were stained with tetramethylrhodamine (TRITC)–conjugated phalloidin and counterstained with DAPI within a 2.5 mg/mL of fibrin matrix incorporating Oregon Green 488–conjugated fibrinogen. Scale bar = 20 μm. These structures evidently have lumens, as demonstrated by confocal images taken at the (**D**) bottom, (**E**) middle, and (**F**) top of a capillary-like formation. These cultures were stained with Oregon Green 488–conjugated phalloidin and counterstained with DAPI and a TRITC-labeled antibody for vinculin. Scale bar = 20 μm.

semiquantitative analysis of active MMPs and their precursors, or zymogens. The resulting data (Fig. 3E–G) demonstrated no significant difference in the early (day 3) activities of MMP-2 and -9 between the measured conditions, with the exception of active MMP-9, which was significantly increased in the cultures comprising 10 mg/mL of fibrinogen.

By day 21, there was virtually uniform expression of all MMPs across these conditions. Western blots demonstrated

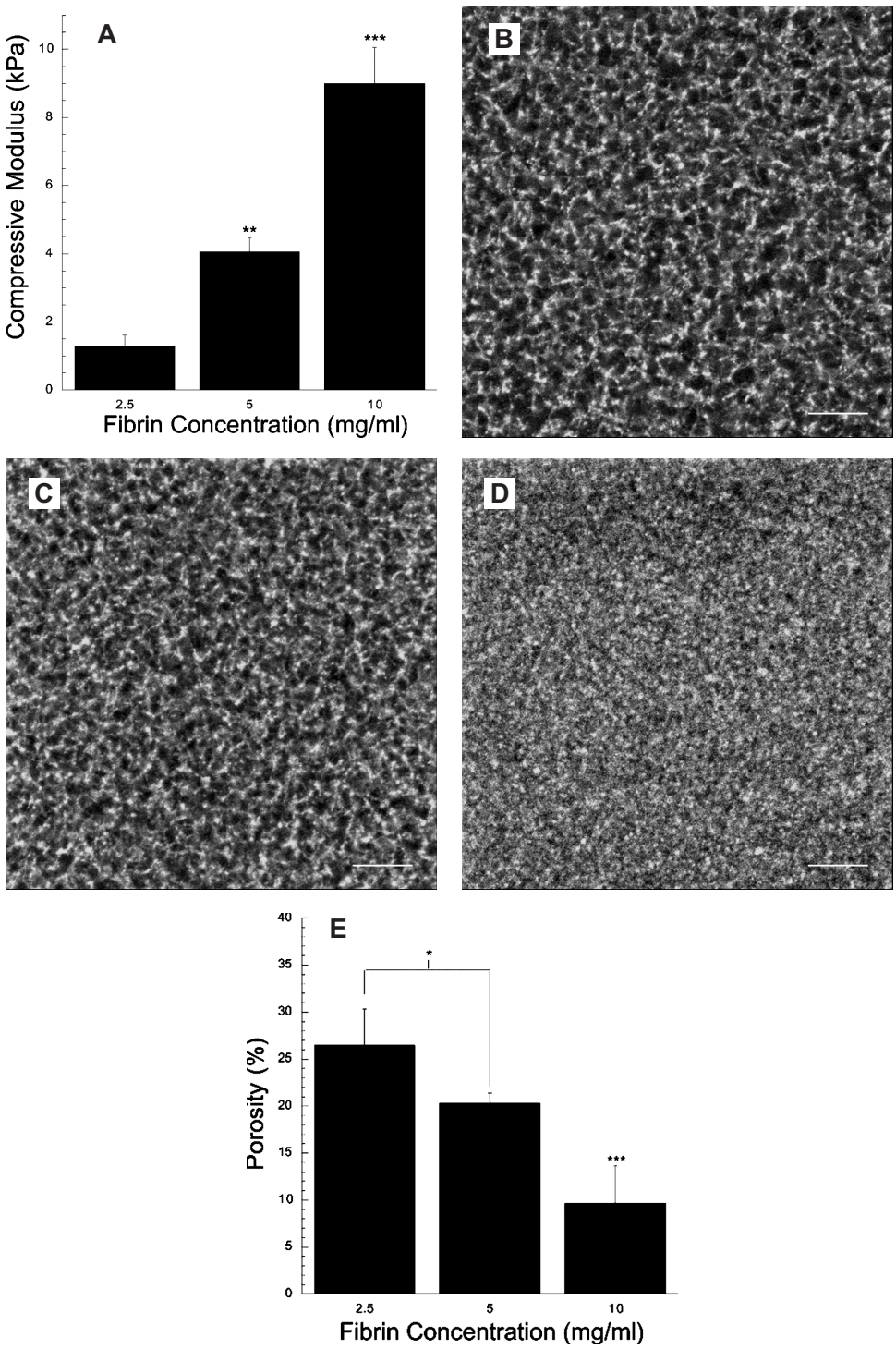

FIG. 2. Compressive modulus and matrix density increase while porosity decreases with greater fibrinogen concentrations. (**A**) Elastic modulus was obtained through unconfined compression testing of fibrin constructs of different concentrations (2.5, 5, and 10 mg/mL). Values presented are an average of 3 samples per condition. ***$p < 0.001$ compared to other samples; **$p < 0.01$ compared to 2.5 mg/mL condition. High-magnification (63×) confocal images were obtained for (**B**) 2.5 mg/mL, (**C**) 5 mg/mL, and (**D**) 10 mg/mL fibrin hydrogels. Gels incorporated a small amount (1:1000) of Oregon Green 488–conjugated fibrinogen added at a concentration commensurate to the bulk gel to allow visualization of the network. Scale bar = 20 μm. (**E**) A total of 5 images per condition were imaged in this fashion and thresholded to obtain a ratio of black to green pixels. The values were averaged and presented as porosity for each fibrin concentration (2.5, 5, and 10 mg/mL). *$p < 0.05$ between the indicated samples; ***$p < 0.001$ when compared to the other 2 samples. Scale bar = 20 μm.

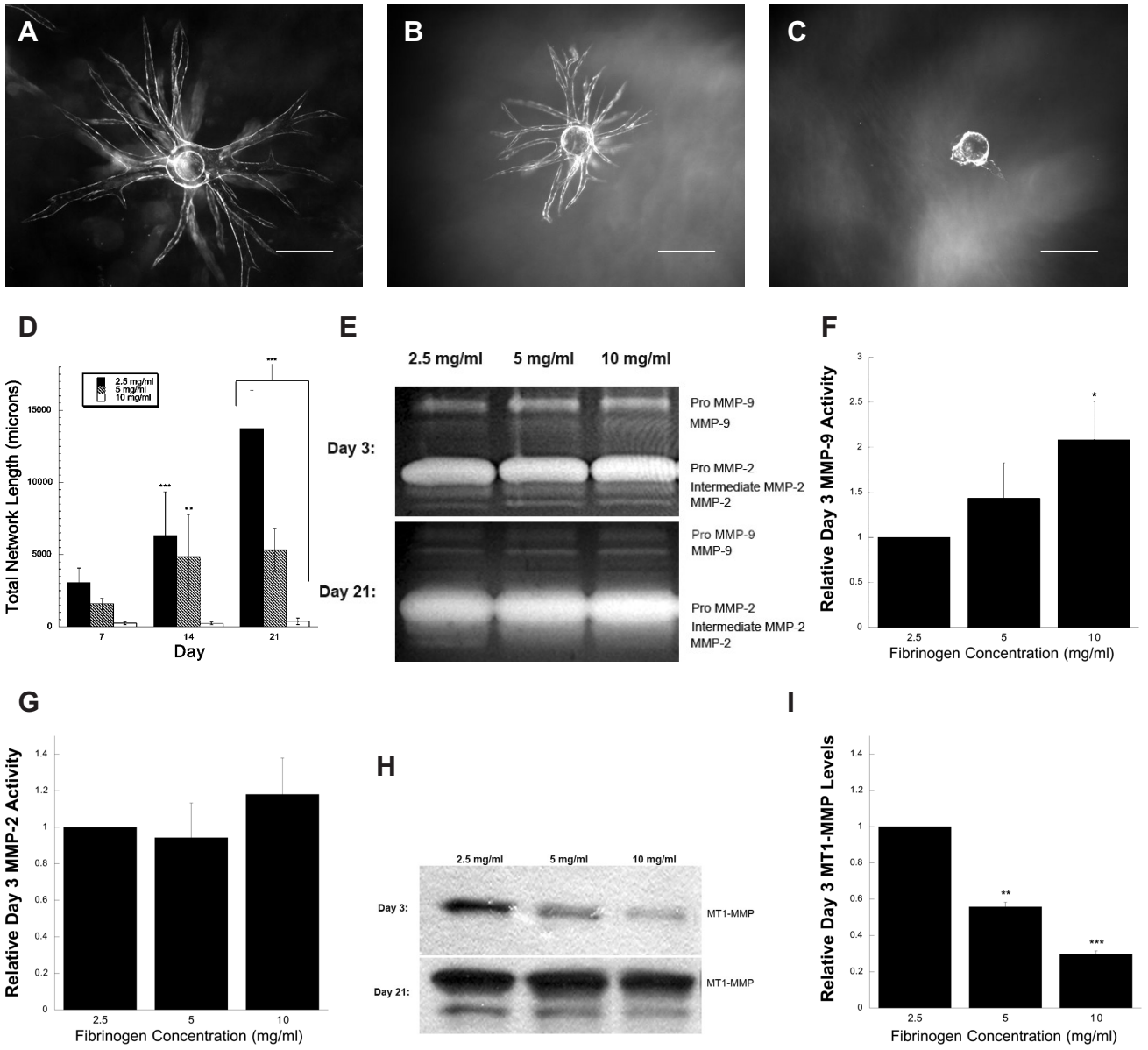

FIG. 3. Increasing fibrin concentration diminishes total network formation, possibly due to reduced early expression of MT1-MMP. Shown are low-magnification (4×) images of representative beads and capillary networks at day 21 within (**A**) 2.5 mg/mL, (**B**) 5 mg/mL, and (**C**) 10 mg/mL fibrin gels used for quantification of total network length. Scale bar = 500 μm. (**D**) At 3 separate time points (days 7, 14, and 21), a total of 5 such beads per condition were quantified for total capillary network length and averaged. $***p < 0.001$; $**p < 0.01$ between samples at the indicated time point. For each condition and time point, 2 gels were digested and pooled to assay for MMP presence and activity via Western blotting and gelatin zymography, respectively. (**E**) Representative images of zymograms ($n = 4$) performed at days 3 and 21 (days 7 and 14 not shown). A standard for MMP-2 and -9 was used to identify bands for pro-MMP-9 (92 kDa), active MMP-9 (88 kDa), pro-MMP-2 (72 kDa), intermediate MMP-2 (64 kDa), and active MMP-2 (62 kDa). Three such images were quantified via scanning densitometry. Resulting quantification of (**F**) active MMP-9 and (**G**) active MMP-2 bands at day 3 are shown. Values presented are normalized within each image by the value for the 2.5 mg/mL culture. $*p < 0.05$ compared to the 2.5 mg/mL condition. (**H**) Representative Western blots ($n = 3$) for samples probed at days 3 and 21 with an antibody for MT1-MMP. Lysates from MCF-7 carcinoma were used as a positive control to identify the relevant band (not shown). (**I**) Two such blots were quantified via scanning densitometry. Day 3 values presented are normalized within each blot by the value obtained for the 2.5 mg/mL condition. $**p < 0.01$ compared to the other 2 conditions; $***p < 0.001$ compared to the low-density condition.

a highly significant decrease in MT1-MMP as matrix density increased at the early time point, ultimately equalizing by day 21 (Fig. 3H, I).

Addition of GM6001 to 2.5 mg/mL cultures mimics the effect of increased matrix density on angiogenic sprouting

We next sought to verify the role played by MMPs in the reduced capillary network formation that occurs with increased matrix density. Accordingly, variable doses (0.1 μM and 1.0 μM) of GM6001, a broad-spectrum inhibitor of secreted MMPs (specifically MMP-1, -2, -3, -8, and -9), were added to the low-density (2.5 mg/mL) tissues (Fig. 4A–C). Network formation of the low-dose condition mirrored that of the 5 mg/mL condition, while increasing the dosage of GM6001 led to network length values approaching those of the 10 mg/mL condition (Figs. 3D and 4D). Surprisingly, the activity of MMP-2 and MMP-9 did not appear significantly altered by the exogenous MMP inhibitor. However, the levels of MT1-MMP at day 3 decreased in a pattern similar to that caused by increasing fibrinogen concentration.

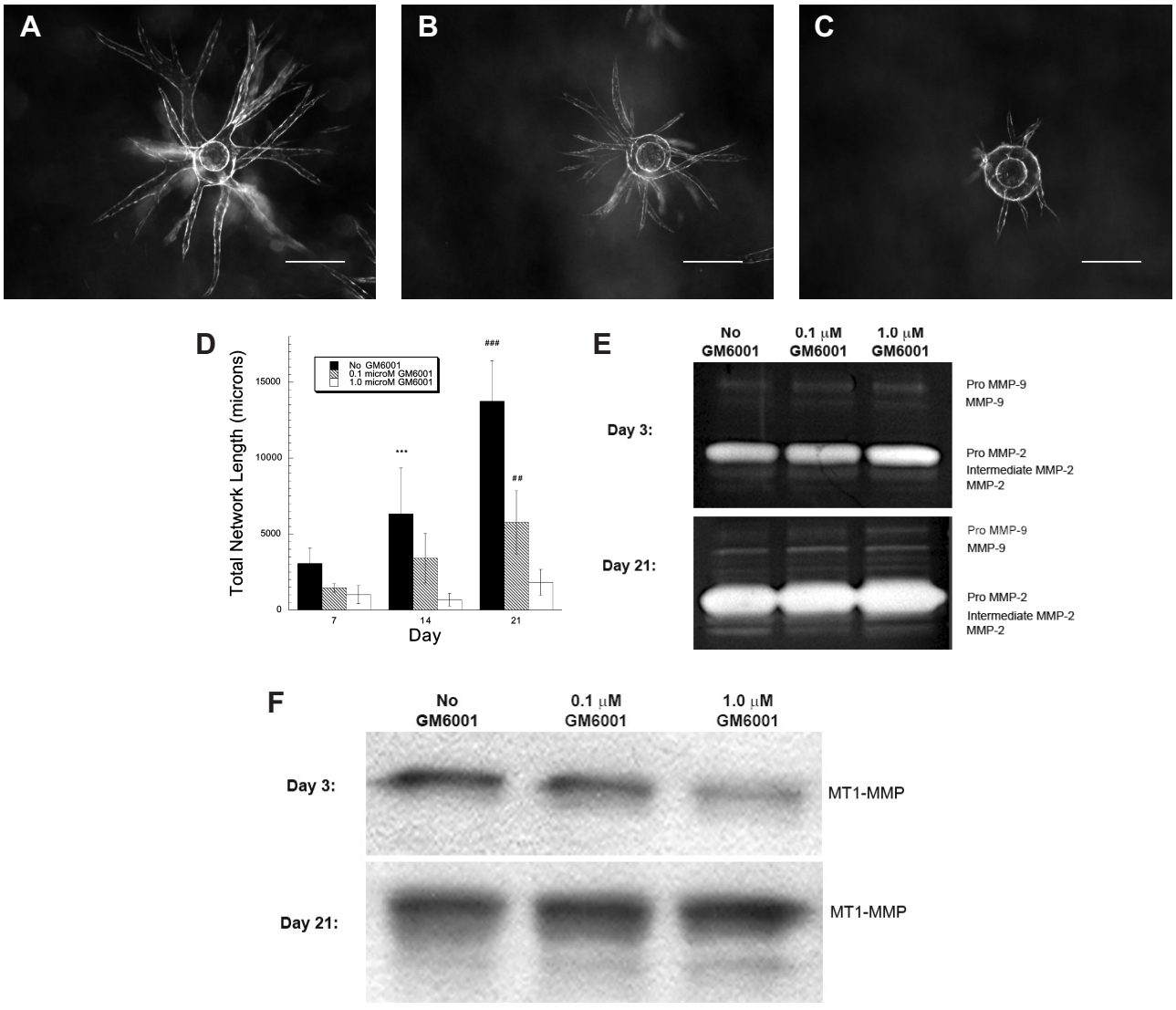

FIG. 4. Total network formation is inhibited in a dose-dependent fashion by GM6001. Low-magnification images (4×) of representative beads and capillary networks at day 21 within 2.5 mg/mL fibrin gels with (**A**) 0 μM, (**B**) 0.1 μM, and (**C**) 1.0 μM exogenous GM6001 used for quantification of total network length. Scale bar = 500 μm. (**D**) At 3 separate time points (days 7, 14, and 21), a total of 5 such beads per condition were quantified for total capillary network length and averaged. ***$p < 0.001$ for the uninhibited condition at day 14 compared to both inhibited conditions; ##$p < 0.01$; ###$p < 0.001$ compared to the maximally inhibited sample at day 21. (**E**) Representative images of zymograms ($n = 4$) performed at days 3 and 21 (days 7 and 14 not shown). (**F**) Representative Western blots ($n = 3$) for samples probed at days 3 and 21 with an antibody for MT1-MMP. Samples were obtained and identified in a manner identical to that described in the caption for Fig. 3.

Incorporation of HMSCs throughout the fibrin matrix increases vascular network formation through a mechanism that may involve early MMP-2, MMP-9, and MT1-MMP upregulation

Because HMSCs can function as pericytes and interact with endothelial cells in coculture,[25] we hypothesized that distributing HMSCs throughout the denser fibrin matrices might influence capillary network formation. Indeed, this was the case by day 21 (Fig. 5A–D). In the 5 mg/mL cultures, inclusion of HMSCs resulted in a nearly 65% increase in total network length (Fig. 5E), more closely approaching the value established in the baseline (2.5 mg/mL) condition. In the 10 mg/mL fibrin gels, the effect of HMSC addition was even more pronounced early and late, culminating in a greater than 7-fold increase in network length by day 21 (Fig. 5F).

Enhanced MMP-2 and -9 activities, along with elevated MT1-MMP levels, were evident early on (i.e., day 3), but were essentially equivalent by day 21. Levels of pro-MMP-9 decreased with the addition of HMSCs, evidently converted to the active form, as HMSC addition coincided with a significant increase in levels of the 88-kDa form in both the 5 and 10 mg/mL cases (Fig. 5G–H). Interestingly all forms of MMP-2 (pro, intermediate, and active) were also more highly expressed in both of the conditions incorporating HMSCs. In fact, HMSC addition resulted in more than double the amount of the most relevant form, active MMP-2, in both 5 and 10 mg/mL cultures (Fig. 5G, I). Examination of MT1-MMP presence revealed a near doubling of levels with the addition of HMSCs in both the 5 mg/mL and 10 mg/mL conditions, but in contrast to MMP-2 and -9 activities, levels of MT1-MMP decreased significantly as matrix density doubled in the mesenchymal cell-containing cultures (Fig. 5J–K).

Inhibition via GM6001 negates the effect of HMSCs on capillary network formation, implicating the importance of MT1-MMP in the process

To confirm that the mechanism behind the increase in capillary network formation caused by the addition of HMSCs is MMP-associated, GM6001 was added to these cultures, again in doses of 0.1 and 1.0 μM. As in the baseline 2.5 mg/mL cultures without HMSCs, GM6001 induced a dose-dependent reduction in sprouting within the 5 mg/mL (Fig. 6A–C) and 10 mg/mL (Fig. 6D–F) conditions containing HMSCs. Quantification of network length in the 5 mg/mL cultures revealed a significant decrease in total network formation with the addition of GM6001 (Fig. 6G). By day 21, the maximally inhibited cultures had a network length amounting to only 19% of the uninhibited case. The 10 mg/mL cultures followed a similar trend; in fact, a maximum dose of the MMP-inhibitor virtually eliminated vascular sprouting at day 7, and led to networks at day 21 that were only 14.4% of the total length of the uninhibited condition (Fig. 6H).

Gelatin zymography revealed no discernable trend involving the expression of MMP-2, MMP-9, or any of their isoforms at any time point in relation to GM6001 dose (Fig. 6I). However, Western blotting showed that the addition of GM6001 to the 5 mg/mL cultures slightly decreased MT1-MMP expression for both dosages at day 3 through day 21 (Fig. 6J). The levels of MT1-MMP in the 10 mg/mL cultures, while unaffected by the addition of GM6001 at day 3, appeared slightly reduced in response to GM6001 addition by day 21.

DISCUSSION

The current study utilizes a stable 3D model of robust angiogenesis to explore the underlying mechanisms of capillary morphogenesis and development in response to altered ECM properties. Increasing the fibrinogen concentration enhances the compressive modulus (Fig. 2A) and decreases the porosity (Fig. 2E) of the matrix, but also severely limits angiogenesis (Fig. 3A–D). The angiogenic response can be recovered in the dense fibrin matrix through the addition of human mesenchymal stem cells (Fig. 5A–F). Our results further demonstrate that an important mechanism underlying these observations is early (< 3 days) upregulation of both soluble (MMP-2 and MMP-9) and membrane-bound (MT1-MMP) MMPs (Fig. 5G–K). The important role of HMSCs and MMPs in promoting angiogenesis may prove useful to the development of angiogenic therapies or the construction of thick, stiff prevascularized tissues.

In the context of prevascularized tissues, the benefit of increasing fibrinogen concentration lies in the creation of tissue constructs with enhanced mechanical properties that can be more easily manipulated *ex vivo* before use *in vivo.* However, our results demonstrate that increased fibrinogen concentration severely limits angiogenesis. Mechanistically, increasing the density of the fibrin matrix does not significantly decrease the activity of MMP-2 and MMP-9, which are soluble and freely diffusible, but does reduce the amount of MT1-MMP (membrane bound). Because increasing the concentration of fibrinogen increases the density of the fibrin matrix while simultaneously increasing the compressive modulus, decreasing the porosity, and increasing the number of matrix binding sites available to membrane-bound integrin receptors, it is difficult to dissect the mechanistic causes for the inhibition of capillary morphogenesis. One possible interpretation is that the nearly 7-fold increase in matrix stiffness increases cytoskeletal tension to alter gene expression within endothelial cells, effectively turning "off" the angiogenic switch[1] that regulates MT1-MMP expression. Alternatively, the increase in binding site density may discourage the cell rounding necessary for tubule formation, instead providing the anchors

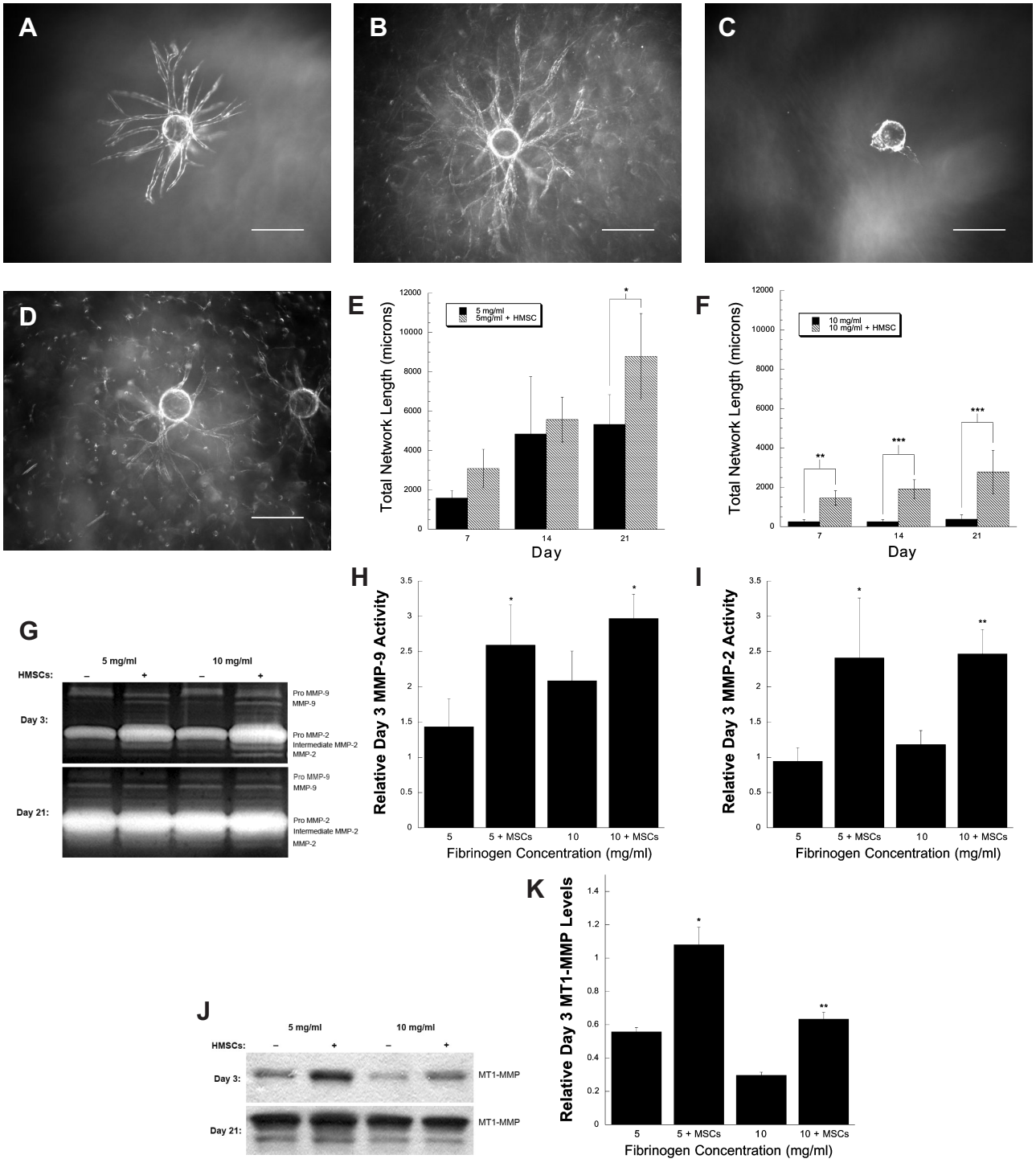

FIG. 5. Total network formation is enhanced within denser fibrin gels by the addition of HMSCs throughout the 3D matrix. Enhanced early expression of MMP-2, MMP-9, and MT1-MMP play a role. Shown are low-magnification images of representative beads and capillary networks at day 21 used for quantification of total network length within (**A, B**) 5 and (**C, D**) 10 mg/mL gels (**A, C**) completely lacking or (**B, D**) containing 50,000 HMSCs dispersed throughout the matrix (white specs throughout the image). Scale bar = 500 μm. At 3 separate time points (days 7, 14, and 21), a total of 5 such beads per condition were quantified and averaged for the (**E**) 5 mg/mL and (**F**) 10 mg/mL samples. $*p < 0.05$; $**p < 0.01$; $***p < 0.001$ between the 2 indicated samples. (**G**) Representative images of zymograms ($n = 4$) performed at days 3 and 21 (days 7 and 14 not shown). Three such images were quantified via scanning densitometry. Resulting quantification of (**H**) active MMP-9 and (**I**) active MMP-2 bands at day 3 are shown. Values presented are normalized within each image by the value for the 2.5 mg/mL culture at this time point (though not shown, a 2.5 mg/mL sample was also run on these gels). $*p < 0.05$ and $**p < 0.01$ compared to the corresponding condition void of HMSCs. (**J**) Representative Western blots ($n = 3$) for samples probed at days 3 and 21 with an antibody for MT1-MMP. Samples were obtained and identified in a manner identical to that described in the caption for Fig. 3. (**K**) Two such blots were quantified by scanning densitometry. Quantification of day 3 MT1-MMP levels are presented normalized to the value obtained for the corresponding 2.5 mg/mL culture (also contained on these blots, though not shown). $*p < 0.05$ compared to the corresponding condition void of HMSCs and the 10 mg/mL condition containing HMSCs. $**p < 0.01$ compared to the corresponding condition void of HMSCs.

and mechanical resistance necessary for cell spreading.[11] The reduction in porosity likely also prevents communication between HUVECs and the overlying fibroblast monolayer via soluble mediators, depriving HUVECs of the soluble cues necessary to fully differentiate. We have previously shown that a maximum distance for HUVEC-fibroblast separation exists, beyond which angiogenesis is essentially eliminated.[7] Ostensibly, this distance is reduced even further in a less porous matrix. Because these individual effects of compressive modulus, porosity, and integrin-matrix binding site density cannot be easily decoupled in gels made from native ECM proteins, deciphering the mechanism responsible for the inhibition of capillary morphogenesis by increased fibrinogen concentration will likely require the use of synthetic ECM analogs capable of controlling each variable independently.[26,27]

From a biotechnology perspective, it is clear from this study that the addition of HMSCs enhances capillary morphogenesis in dense fibrin matrices. Mechanistically, our results suggest that HMSCs upregulate the expression of MT1-MMP, MMP-2, and MMP-9 within the culture system by day 3 (Fig. 5G–K), and that this early upregulation sustains enhanced network formation. However, MT1-MMP appears to have a significant role. Although the 10 mg/mL cultures containing HMSCs do not have appreciably different MMP-2 and -9 activity when compared to their 5 mg/mL counterparts, the functional output of total network length is still far less in the 10 mg/mL cultures. MT1-MMP levels, on the other hand, reflect this trend, as they decrease with matrix density in the mesenchymal cell–containing cultures. Inhibition studies performed by adding GM6001 to the HMSC-containing matrices further suggest an essential role for the membrane-associated MMP. Specifically, while the addition of GM6001 resulted in a significant decrease in network formation (Fig. 6A–H), levels of active MMP-2 and -9 were not altered in a similar pattern (Fig. 6I). Instead, the noted decrease in network formation coincided with a decrease in MT1-MMP levels (Fig. 6J).

While the affinity of GM6001 for MT1-MMP has yet to be established,[28] the downregulation of MT1-MMP levels in its presence is plausible given the structural similarities of MMPs and the co-regulation of MT1-MMP and MMP-2 expression.[29] Our result is also consistent with studies describing the particular importance of MT1-MMP in matrix invasion and vessel formation by endothelial cells.[17,30] A diverse and potent protease, MT1-MMP not only activates MMP-2,[31] but it also has greater fibrinolytic capability than MMP-2 or -9[17] and can be released in an active, soluble form from the cellular membrane into the surrounding matrix.[32] These functions bestow MT1-MMP with the ability to act in a highly local fashion to mediate ECM degradation pericellularly, partly to release matrix-bound growth factors important for angiogenesis exactly where needed.[23] The pericellular role of MT1-MMP could prove particularly important to the initiation of capillary formation, as spatial coordination of MMP activity may prove more important than bulk levels of activity. Understanding the precise role played by MT1-MMP in angiogenesis will prove useful in the development of angiogenic therapies and guide the design of more mechanically viable prevascularized tissues.

While these data suggest that HMSCs enhance angiogenesis within denser matrices partly through increasing MT1-MMP levels, the precise mechanism by which network length is enhanced is not known. Recent studies have highlighted the ability of these cells to form capillary-like structures on their own.[33] Though unlikely, given that the culture conditions shown to induce HMSC differentiation to an endothelial-like phenotype do not match those of this study, it is possible that HMSCs are contributing to the enhanced network lengths observed by differentiating into endothelial cells and incorporating into the growing network.[33]

Recent evidence also implicates endothelial cell–mesenchymal cell crosstalk. Endothelial cells have been shown to attract undifferentiated mesenchymal cells through paracrine mechanisms.[25] While the exact mechanism for how HMSCs would enhance bulk MT1-MMP levels through this fashion is unclear, there is also a growing body of evidence that implies needy cells (e.g., HUVECs stimulated by proangiogenic factors) shed a membrane protein called EMMPRIN (extracellular matrix metalloproteinase inducer) to induce production of MMPs by stromal cells.[31] Thus, the mechanism by which bulk MT1-MMP levels are enhanced by 3D distribution of HMSCs throughout the denser matrices may simply be based on the reduction in distance that pericyte-secreted cytokines must diffuse, as previously discussed. Generally, distributing an interstitial cell throughout the matrix may allow for more effective crosstalk between HUVECs and the stromal cell via soluble mediators (e.g., EMMPRIN, VEGF, etc.). Specifically, in the case of HMSCs, this paracrine signaling could then lead to increased production of latent MMP-2 and -9 by the HMSCs. These zymogens could then diffuse freely to the HUVEC surface owing to the reduced diffusion distances, where they are activated locally by the HUVEC MT1-MMP. In fact, the enhanced presence of latent MMP-2 may result in increased intracellular production and processing of MT1-MMP to the HUVEC surface. Active MMP-2 is capable of activating MMP-9 in turn.[30] Ultimately, not only would the bulk levels of these proteases increase, but their spatial distribution would ostensibly be optimized, allowing a greater amount of active MMPs to be utilized locally by the HUVECs. This would account for the increased sprouting that occurred within the dense matrices in the presence of HMSCs.

The observed increase in vascular network formation as a result of HMSC addition may also involve the upregulation of other proteolytic enzymes. MT2-MMP and MT3-MMP have implicated roles in angiogenesis,[30,34] as does the plasmin/plasminogen activator system of serine

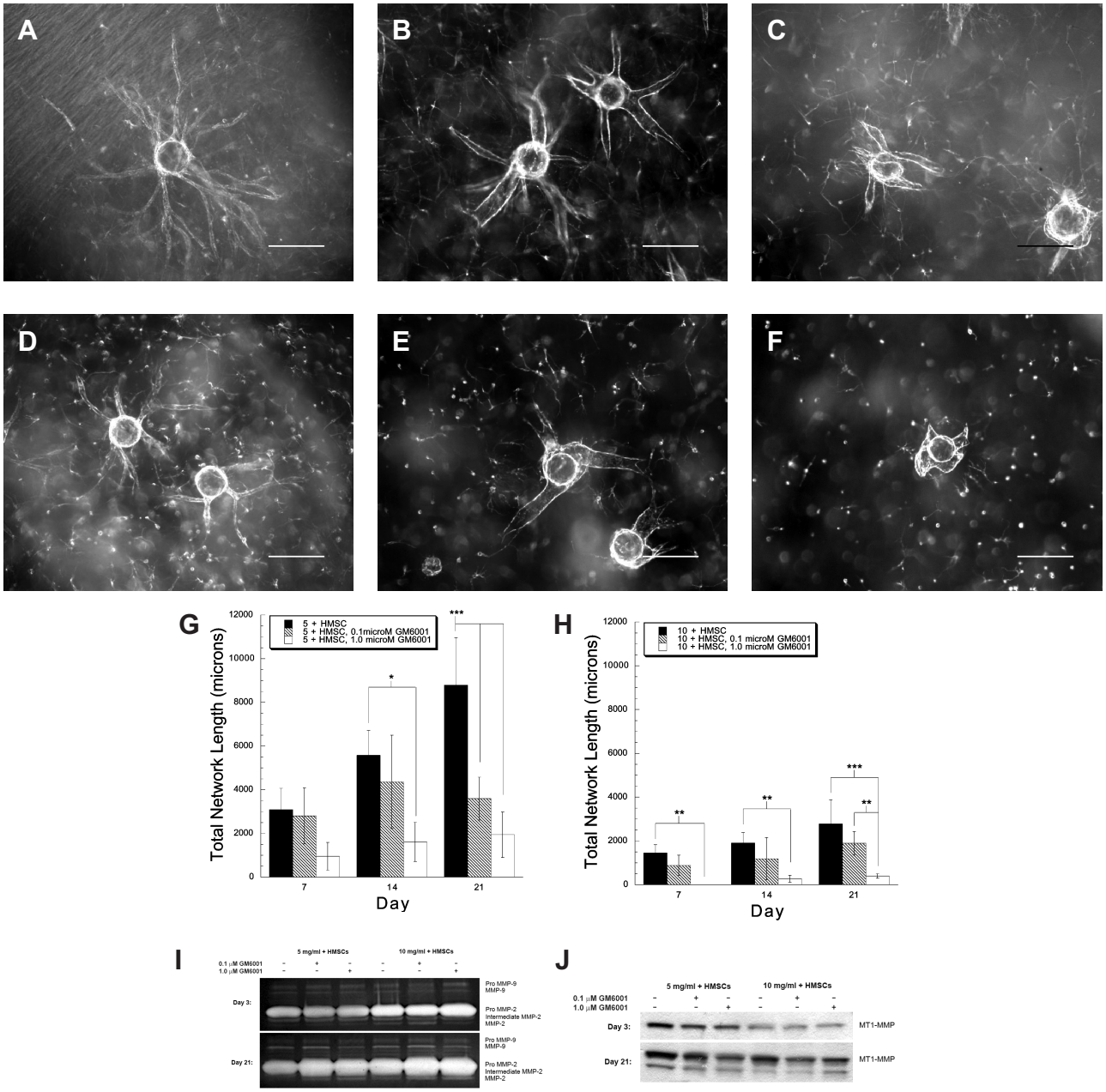

FIG. 6. Total network formation is again inhibited by GM6001 in a dose-dependent manner within fibrin matrices containing HMSCs. Low-magnification images of representative beads and capillary networks at day 21 indicative of those used for quantification of total network length within (**A–C**) 5 and (**D–F**) 10 mg/mL gels containing HMSCs distributed throughout the matrix with (**A, D**) 0 μM; (**B, E**) 0.1 μM; and (**C, F**) 1.0 μM exogenous GM6001 added. Scale bar = 500 μm. At 3 separate time points (days 7, 14, and 21), a total of 5 such beads per condition were quantified and averaged for the (**G**) 5 mg/mL conditions and (**H**) 10 mg/mL conditions. $*p < 0.05$, $**p < 0.01$, and $***p < 0.001$ between the 2 indicated samples. (**I**) Representative images of zymograms ($n = 4$) performed at days 3 and 21 (days 7 and 14 not shown). (**J**) Representative Western blots ($n = 3$) for samples probed at days 3 and 21 with an antibody for MT1-MMP. Samples were obtained and identified in a manner identical to that described in the caption for Fig. 3.

proteases.[18,35] Future work will determine how the levels of these molecules are affected by HMSC addition.

In conclusion, the present work demonstrates the ability of HMSCs to enhance angiogenesis within dense fibrin tissues. Early production of MMPs, including soluble forms (MMP-2 and -9) as well as membrane-bound (MT1-MMP), are part of the underlying mechanism, suggesting that both interstitial cell signaling and pericellular control of proteolytic activity are crucial steps in angiogenesis. These results may prove useful in the design of engineered prevascularized tissues by enhancing the tissue mechanical properties while maintaining function, thus yielding a tissue

that is more easily manipulated *ex vivo*. Further, the results provide a basis for the application of HMSCs in angiogenic therapies to enhance vascular growth into ischemic tissues.

ACKNOWLEDGMENTS

This project was supported in part by a grant to S.C.G. from the National Institutes of Health (R01 HL-067954), by seed grants to S.C.G. from the Council on Research, Computing, and Library Resources (CORCLR) and the Department of Biomedical Engineering at the University of California, Irvine, as well as setup funds provided to A.J.P. from the University of California, Irvine. We would like to acknowledge Mr. Chirag Khatiwala, Mr. Craig Griffith, and Dr. Zifu Wang for graciously lending their technical assistance.

REFERENCES

1. Ingber, D.E., and Folkman, J. How does extracellular matrix control capillary morphogenesis? Cell **58,** 803, 1989.
2. Jain, R.K., Schlenger, K., Hockel, M., and Yuan, F. Quantitative angiogenesis assays: progress and problems. Nat. Med. **3,** 1203, 1997.
3. Lafleur, M.A., Handsley, M.M., Knauper, V., Murphy, G., and Edwards, D.R. Endothelial tubulogenesis within fibrin gels specifically requires the activity of membrane-type-matrix metalloproteinases (MT-MMPs). J. Cell Sci. **115,** 3427, 2002.
4. Jain, R.K. Molecular regulation of vessel maturation. Nat. Med. **9,** 685, 2003.
5. Brey, E.M., Uriel, S., Greisler, H.P., and McIntire, L.V. Therapeutic neovascularization: contributions from bioengineering. Tissue Eng. **11,** 567, 2005.
6. Jain, R. K., Au, P., Tam, J., Duda, D. G., and Fukumara, D. Engineering vascularized tissue. Nat. Biotechnol. **23,** 821, 2005.
7. Griffith, C., Miller, C., Sainson, R., Calvert, J., Jeon, N., Hughes, C., and George, S. Diffusion limits of an in vitro thick prevascularized tissue. Tissue Eng. **1–2,** 257, 2005.
8. Koike, N., Fukumura, D., Gralla, O., Au, P., Schechner, J. S., and Jain, R.K. Tissue engineering: creation of long-lasting blood vessels. Nature **428,** 138, 2004.
9. Levenberg, S., Rouwkema, J., Macdonald, M., Garfein, E.S., Kohane, D.S., Darland, D.C., Marini, R., Blitterswijk, C.A. v., Mulligan, R.C., D'Amore, P.A., and Langer, R. Engineering vascularized skeletal muscle tissue. Nat. Biotechnol. **23,** 879, 2005.
10. Enis, D.R., Shepherd, B.R., Wang, Y., Qasim, A., Shanahan, C.M., Weissberg, P. L., Kashgarian, M., Pober, J.S., and Schechner, J.S. Induction, differentiation, and remodeling of blood vessels after transplantation of Bcl-2-transduced endothelial cells. Proc. Natl. Acad. Sci. **102,** 425, 2005.
11. Ingber, D.E., and Folkman, J. Mechanochemical switching between growth and differentiation during fibroblast growth factor-stimulated angiogenesis in vitro: role of the extracellular matrix. J. Cell Biol. **109,** 317, 1989.
12. Vailhe, B., Lecomte, M., Wiernsperger, N., and Tranqui, L. The formation of tubular structures by endothelial cells is under the control of fibrinolysis and mechanical factors. Angiogenesis **2,** 331, 1998/1999.
13. Urech, L., Bittermann, A.G., Hubbell, J.A., and Hall, H. Mechanical properties, proteolytic degradability and biological modifications affect angiogenic process extension into native and modified fibrin matrices in vitro. Biomaterials **26,** 1369, 2005.
14. Sieminiski, A.L., Hebbel, R.P., and Gooch, K.J. The relative magnitudes of endothelial force generation and matrix stiffness modulate capillary morphogenesis in vitro. Exp. Cell Res. **297,** 574, 2004.
15. Nehls, V., and Drenckhahn, D. A novel, microcarrier-based in vitro assay for rapid and reliable quantification of three-dimensional cell migration and angiogenesis. Microvasc. Res. **50,** 311, 1995.
16. Nakatsu, M.N., Sainson, R.C.A., Aoto, J.N., Taylor, K.L., Aitkenhead, M., Perez-del-Pulgar, S., Carpenter, P.M., and Hughes, C.C.W. Angiogenic sprouting and capillary lumen formation modeled by human umbilical vein endothelial cells HUVEC in fibrin gels: the role of fibroblasts and angiopoietin-1. Microvasc. Res. **66,** 102, 2003.
17. Hiraoka, N., Allen, E., Apel, I.J., Gyetko, M.R., and Weiss, S.J. Matrix metalloproteinases regulate neovascularization by acting as pericellular fibrinolysins. Cell **95,** 365, 1998.
18. Collen, A., Hanemaaijer, R., Lupu, F., Quax, P.H.A., Lent, N. v., Grimbergen, J., Peters, E., Koolwijk, P., and Hinsbergh, V.W.M. v. Membrane-type matrix metalloproteinase-mediated angiogenesis in a fibrin-collagen matrix. Blood **101,** 1810, 2003.
19. Robinet, A., Fahem, A., Cauchard, J.-H., Huet, E., Vincent, L., Lorimier, S., Antonicelli, F., Soria, C., Crepin, M., Hornebeck, W., and Bellon, G. Elastin-derived peptides enhance angiogenesis by promoting endothelial cell migration and tubulogenesis through upregulation of MT1-MMP. J. Cell Sci. **118,** 343, 2005.
20. Anseth, K.S., Bowman, C.N., and Brannon-Peppas, L. Mechanical properties of hydrogels and their experimental determination. Biomaterials **17,** 1647, 1996.
21. Dubey, N., Letourneau, P.C., and Tranquillo, R.T. Neuronal contact guidance in magnetically aligned fibrin gels: effect of variation in gel mechano-structural properties. Biomaterials **22,** 1065, 2001.
22. Clark, R.A.F. Overview of wound repair. In: Clark, R.A.F., ed. The Molecular and Cellular Biology of Wound Repair. New York: Plenum Press, 1995, p. 24.
23. Mott, J.D., and Werb, Z. Regulation of matrix biology by matrix metalloproteinases. Curr. Opin. Cell Biol. **16,** 558, 2004.
24. Engler, A.J., Griffin, M.A., Sen, S., Bonnemann, C.G., Sweeney, H.L., and Discher, D.E. Myotubes differentiate optimally on substrates with tissue-like stiffness: pathological implications for soft or stiff microenvironments. J. Cell Biol. **166,** 877, 2004.
25. Hirschi, K., Rohovsky, S., and D'Amore, P. PDGF, TGF-beta, and heterotypic cell-cell interactions mediate endothelial cell-induced recruitment of 10T1/2 cells and their differentiation to a smooth muscle fate. J. Cell Biol. **141,** 805, 1998.
26. Raeber, G.P., Lutolf, M.P., and Hubbell, J.A. Molecularly engineered PEG hydrogels: a novel model system for pro-

teolytically mediated cell migration. Biophys. J. **89,** 1374, 2005.
27. Almany, L., and Seliktar, D. Biosynthetic hydrogel scaffolds made from fibrinogen and polyethylene glycol for 3D cell cultures. Biomaterials **15,** 2467, 2005.
28. Grobelny, D., Poncz, L., and Galardy, R.E. Inhibition of human skin fibroblast collagenase, thermolysin, and *Pseudomonas aeruginosa* elastase by peptide hydroxamic acids. Biochemistry **31,** 7152, 1992.
29. Sternlicht, M.D., and Werb, Z. How matrix metalloproteinases regulate cell behavior. Annu. Rev. Cell. Dev. Biol. **17,** 463, 2001.
30. Chun, T.-H., Sabeh, F., Ota, I., Murphy, H., McDonagh, K.T., Holmbeck, K., Birkedal-Hansen, H., Allen, E.D., and Weiss, S.J. MT1-MMP-dependent neovessel formation within the confines of the three-dimensional extracellular matrix. J. Cell Biol. **167,** 757, 2004.
31. Bausbaum, C.B., and Werb, Z. Focalized proteolysis: spatial and temporal regulation of extracellular matrix degradation at the cell surface. Curr. Opin. Cell Biol. **8,** 731, 1996.
32. Toth, M., Osenkowski, P., Hesek, D., Brown, S., Meroueh, S., Sakr, W., Mobashery, S., and Fridman, R. Cleavage at the stem region releases an active ectodomain of the membrane type 1 matrix metalloproteinase. Biochem. J. **387,** 497, 2005.
33. Annabi B., Lee Y., Turcotte S., Naud E., Desrosiers R., Champagne M., Eliopoulos N., Galipeau J., and Beliveau R. Hypoxia promotes murine bone-marrow-derived stromal cell migration and tube formation. Stem Cells **21,** 337, 2005.
34. Plasier, M., Kapiteijn, K., Koolwijk, P., Fijten, C., Hanemaaijer, R., Grimbergen, J.M., Mulder-Stapei, A., Quax, P.H.A., Helmerhorst, F.M., and Hinsbergh, V.W.M. v. Involvement of membrane-type matrix metalloproteinases (MT-MMPs) in capillary tube formation by human endometrial microvascular endothelial cells: role of MT3-MMP. J. Endocrinol. Metab. **89,** 5828, 2004.
35. Kroon, M.E., Koolwijk, P., Goor, H. v., Weidle, U.H., Collen, A., Pluijm, G. v. d. and Hinsbergh, V.V.M. v. Role and localization of urokinase receptor in the formation of new microvascular structures in fibrin matrices. Am. J. Pathol. **154,** 1731, 1999.

Address reprint requests to:
Andrew J. Putnam, Ph.D.
Department of Chemical Engineering and Materials Science
916 Engineering Tower
University of California, Irvine
Irvine, CA 92697-2575

E-mail: aputnam@uci.edu